THE ASTROPHYSICAL JOURNAL, 229:713–727, 1979 April 15

NUCLEAR FORCES, PARTITION FUNCTIONS, AND DISSOCIATION IN STELLAR COLLAPSE*

T. J. MAZUREK
Department of Astronomy, University of Texas at Austin
JAMES M. LATTIMER
Department of Astronomy, University of Illinois at Urbana-Champaign
AND
G. E. BROWN
Nordita, Copenhagen, Denmark; and State University of New York at Stony Brook
Received 1978 June 19; accepted 1978 October 31

ABSTRACT

Current work on the dynamic collapse of stellar cores indicates that dissociation of the heavy nuclei is a critical factor in determining whether the outcome can be a supernova. A large fraction of the matter is in the form of heavy nuclei even at densities exceeding 10^{13} g cm^{-3}. A number of physical processes become important for the dissociation of the heavy nuclei at these high densities. Sufficient free nucleons are present that the effects of nuclear forces between them become significant. The conditions are such that the partial degeneracy of the neutrons cannot be neglected. The nuclei are in highly excited states, and their partition functions become large. The Coulomb lattice energy is also included in our considerations. The effects of these various processes on nuclear dissociation are examined. All of these processes except the Coulomb lattice energy have large effects on the temperature of nuclear dissociation for densities above 10^{13} g cm^{-3}. With increasing density the dissociation temperature levels off at $\sim 1.1 \times 10^{11}$ K when the density becomes greater than $\sim 5 \times 10^{13}$ g cm^{-3}. Implications of these results for stellar collapse calculations are discussed.

Subject headings: dense matter — nuclear reactions — stars: collapsed

I. INTRODUCTION

In the final stage of evolution, stars with masses above $\sim 8\ M_\odot$ are expected to develop electron-degenerate cores of $\sim 1.4\ M_\odot$ consisting of iron-peak elements (Arnett 1973). The combined effects of nuclear dissociation and electron capture then destabilize the core and lead to stellar collapse. A supernova may result if a significant fraction of the gravitational energy of collapse is deposited in the outer regions of the star (Colgate and White 1966). However, the most recent numerical studies (Arnett 1977; Wilson 1977; Mazurek 1979) have given ambiguous results regarding the outcome. Somewhat different assumptions regarding the input physics can give an explosion (Wilson 1977) or total collapse (Mazurek 1979). The greatest uncertainty, perhaps, lies in the equation of state.

Throughout the collapse the pressure is dominated by the leptons (electrons and electron neutrinos) and the free neutrons. Initially, the relativistically degenerate electrons overwhelmingly dominate the pressure. Electron capture thus plays a crucial role in destabilizing the core. As the densities exceed $\sim 10^{11}$ g cm^{-3}, the neutrinos from the electron capture become trapped (Mazurek 1976; Yueh and Buchler 1977; Arnett 1977; Tubbs 1978). The neutrino concentration grows until beta equilibrium between electron capture and neutrino absorption is established at densities around 10^{12} g cm^{-3}. Beyond this the concentration of the degenerate leptons remains roughly constant, being depleted only by the relatively slow process of neutrino diffusion. The leptonic pressure now increases more rapidly with density; however, it alone cannot prevent further collapse. Since the leptons are relativistic, their adiobatic index is 4/3 and their pressure alone cannot stabilize the core. The nonleptonic pressure of the massive particles must therefore reverse the core's collapse or cause it to bounce.

The magnitude of the nonleptonic pressure is sensitive to the dissociation of the heavy nuclei. Although dissociation absorbs thermal energy, it also increases the number density of the heavy particles. There is therefore a tendency to enhance the pressure contribution of the nonleptonic component as dissociation increases the particle densities. Because of the competing decrease in pressure due to the absorption of thermal energy it is not possible to determine the growth of the nonleptonic pressure without detailed numerical calculations. But its enhancement

* Supported in part by NSF (grant AST 76-07629) at the University of Texas at Austin and by USDOE (contract EY-76-S-02-3001) at the University of New York at Stony Brook.

is determined by the mode of dissociation of the nuclei; hence, so is the point at which the bounce of the core occurs.

The central density of the core at bounce apparently determines whether an explosion can result. Wilson's (1977) calculations, which give a core bounce at central densities around 10^{13} g cm^{-3}, produce an explosion. Mazurek's (1979) calculations show a core bounce at $\sim 10^{14}$ g cm^{-3} and result in total collapse. The differences between the equations of state used may account for the differing results.

This communication examines the uncertainties in the equation of state that arise from the dissociation of the heavy nuclei. This problem has been investigated by Lattimer and Ravenhall (1978). They formulate it in the context of a coexistence of two different nuclear phases, where the denser phase represents the existence of nuclei. Our approach to the problem of dissociation is quite similar to that using the usual Saha equation (cf., e.g., Burbidge *et al.* 1957). We incorporate the effects of nuclear and Coulomb forces, as well as the partial degeneracy of the free nucleons, through correction terms to the binding energy of each nucleus. The nuclear partition functions appear explicitly, and the equilibrium composition is determined on the basis of a network of discrete nuclei. The relative importance of each physical process can be examined individually.

In particular, we define dissociation curves in the (ρ, T)-plane by requiring that half of the matter be in the form of free nucleons. We then examine the changes in the dissociation curves that are effected by inclusion of the nuclear partition functions, the partial degeneracy of and the nuclear interaction between the free nucleons, and the Coulomb lattice energy. Section II presents our simplified method for incorporating these effects in a Saha like formalism. Section III presents dissociation curves, examines the relative importance of the various processes, and discusses the implications for calculations of hydrodynamic collapse.

II. EQUILIBRIUM WITH INTERACTING NUCLEONS

The equilibrium composition of the matter is obtained by minimizing the total Helmholtz free energy with respect to composition. The difficulty in this approach lies in determining the functional form of the free energy. In this investigation we do not attempt a rigorous derivation of the latter. Rather, we make simplifying assumptions to arrive at a plausible form, and use the result in the following section to examine possible effects on the equation of state in stellar collapse.

Differences in the interactions between individual constituents make the free energy depend on the composition of the matter, as well as its temperature and density. We assume that the free energy of each constituent can be expressed as a sum of its usual noninteracting term plus separate contributions due to Coulomb and nuclear interactions. For the noninteracting free energies we use the expressions of a relativistic Fermi gas for the leptons, a Boltzmann gas for the nuclei, and a nonrelativistic Fermi gas for the nucleons. Minimization of the free energy with respect to the composition of each constituent then yields interacting chemical potentials with relations describing the nuclear and beta equilibria. The nuclear equilibrium condition for the nuclei and nucleons is then expressed in a Saha form with an effective binding energy of a nucleus that allows for nucleon degeneracy, and for both nuclear and Coulomb forces.

a) Coulomb Energy

A detailed study of the thermodynamic properties of a one-component plasma has been presented by Hansen (1973). The total free energy of the ion gas is expressible as a sum of two terms: that of a Boltzmann gas and a Coulomb interaction contribution. The Coulomb portion per ion particle is a product of k_BT (Boltzmann's constant times the temperature) and a dimensionless function $Q_z(a_z k_B T)/k_B T$ that depends on the parameter

$$\Gamma_z(a_z k_B T) = \frac{1}{k_B T}\left(\frac{e^2 z^2}{a_z}\right) = \frac{e^2 z^{5/3}}{k_B T}\left(\frac{4\pi}{3} X_e N_0 \rho\right)^{1/3}, \tag{1}$$

where e is the charge of an electron, Z the proton number of the ion, a_z the ion-sphere radius, X_e the electron number per gram of matter in units of Avogadro's number N_0, and ρ is the mass density. Hansen's Monte Carlo results for the dimensionless function are fitted to within 10% by

$$\frac{Q_z(a_z k_B T)}{k_B T} \cong -\frac{0.9\Gamma_z(a_z k_B T)}{[1 + 4/\Gamma_z(a_z k_B T)]^{1/2}}, \tag{2}$$

The Coulomb free energy per gram is then

$$f_{\rm Coul} \approx N_0 Q_z(a_z k_B T)/A, \tag{3}$$

where A is the mass number of the nucleus. Note that $Q_z(a_z k_B T)$ reduces to the Coulomb energy of a Wigner-Seitz sphere as $\Gamma_z(a_z k_B T) \to \infty$, and is roughly the energy per ion in the Debye-Hückel theory for $\Gamma_z(a_z k_B T) \ll 1$. For the multicomponent plasma of interest we assume that each component contributes a Coulomb interaction term to the free energy of the form given by equation (3).

b) Nuclear Interaction Energy

As the density becomes sufficiently high, the short-range nuclear forces become important for the free neutrons that are present. The particle densities of nuclei are lower than those of the neutrons by factors of roughly A^{-1}. Because of the higher particle densities of the free neutron gas, its self-interaction gives the dominant contribution to the nuclear free energy. The presence of free protons increases the interaction energy of the neutron gas. The free-nucleon contribution therefore is a function of both the nucleon density and the free proton fraction. The main effect of the free nucleons on the nuclei is to reduce surface energies and hence to increase the nuclear binding energies. In the numerical results below, only the self-interaction of the free nucleons is accounted for. The thermodynamic properties of interacting nucleons at finite temperatures have been studied by Buchler and Coon (1977), El Eid and Hilf (1977), and Bowers, Gleeson, and Wheeler (1977). They present numerical results of the thermodynamic properties of the nucleon gas, but each calculation either fixes the proton fraction *a priori* or determines it on the basis of beta equilibrium without accounting for nuclei or neutrino trapping. Thus these results cannot be used readily to derive the nucleon free energy due to nuclear interaction. For expediency, we adopt the bulk interaction energy at zero temperature (as given by Baym, Bethe, and Pethick 1971, and modified by Mackie 1976) for this free energy. The interaction energy per gram ($f_{\rm nuc}$) of free nucleons is then given by

$$f_{\rm nuc} = N_0 W(k, \beta)\,, \tag{4}$$

with $k^3 = 1.5\pi^2 N_0(X_{1,1} + X_{1,0})\rho$ and $\beta = X_{1,1}/(X_{1,1} + X_{1,0})$, where $X_{1,1}$ and $X_{1,0}$ are the mass fractions of free protons and neutrons, respectively, and the functional form of W as modified by Mackie (1976) is given in the Appendix. An explicit form for the binding energy of a nucleus in a sea of free nucleons is not presently available. We assume a function of the form $B_{Z,A}(X_{1,1}, X_{1,0})$, which becomes the usual binding energy of a nucleus $B_{Z,A}{}^0$ in the limit $X_{1,1} + X_{1,0} \to 0$.

c) Helmholtz Free Energy

The contribution of each constituent to the total free energy is $F_i = X_i f_i$ where X_i is its fraction by mass and f_i its free energy per gram. Using the notation

$$\langle a \rangle \equiv \sum_{A,Z} X_{A,Z} a_{A,Z}\,, \tag{5}$$

where the sum is taken over all nuclei and nucleons, one can write the total free energy per gram as

$$f = \langle f^0 + N_0 E \rangle + F_e{}^0 + F_\nu{}^0\,, \tag{6}$$

where for $A > 1$ the interaction energy is

$$E_{A,Z} = (B_{A,Z} + Q_Z)/A\,; \tag{7}$$

and for the nucleons

$$E_{1,1} = W + Q_1\,, \tag{8}$$

$$E_{1,0} = W\,. \tag{9}$$

The superscript zero indicates the appropriate free energies for noninteracting particles. Equation (6) implicitly contains X_ν, the neutrino number per gram in units of N_0, and f_ν, the free energy of N_0 neutrinos. The electron contribution is described similarly.

d) Zeroth-Order Chemical Potentials

For equal mass fractions, the particle density of a nucleus is down by a factor of A from that of the nucleons. Since the neutrons become only partially degenerate in current calculations, the chemical potential of a nucleus should be nearly that of a Boltzmann gas,

$$\exp\left(\mu_{A,Z}{}^B/k_{\rm B}T\right) = \frac{n_{A,Z}}{\Omega_{A,Z}}\left(\frac{h^2 N_0}{2\pi k_{\rm B} T A}\right)^{3/2}\,, \tag{10}$$

where h is Planck's constant, $n_{A,Z} = X_{A,Z} N_0 \rho / A$, and $\Omega_{A,Z}$ is the internal partition function of the nucleus. The nucleons can become partially degenerate, so their chemical potential must be determined on the basis of a Fermi gas. Since they remain nonrelativistic throughout, their chemical potential satisfies (cf., e.g., Chiu 1968)

$$\frac{2}{\sqrt{\pi}}\int_0^\infty \frac{y^{1/2}dy}{\exp\left(y - \mu_{1,Z}{}^0/k_{\rm B}T\right) + 1} = \frac{n_{1,Z}}{\Omega_{1,Z}}\left(\frac{h^2 N_0}{2\pi k_{\rm B} T}\right)^{3/2}\,, \tag{11}$$

where $\Omega_{1,1} = \Omega_{1,0} = 2$. The electrons are extremely relativistic, so their rest mass is negligible. Both the neutrinos

and the electrons are degenerate, so the Fermi expression for their chemical potentials must be used. For the relativistic leptons, the chemical potentials are given by

$$4\pi \int_0^\infty \frac{y^2 dy}{\exp(y - \mu_i^0/k_B T) + 1} = \frac{X_i N_0 \rho}{\Omega_i} \left(\frac{hc}{k_B T}\right)^3 , \tag{12}$$

where i denotes the electron or the neutrino, c is the speed of light, and $\Omega_\nu = \frac{1}{2}\Omega_e = 1$, since helicity distinguishes the antiparticle nuetrino from the particle one.

e) *Equilibrium Composition*

The composition of equilibrium matter is obtained by minimization of f at constant ρ and T subject to charge neutrality and the conservation of baryon and lepton numbers. This standard procedure results in relations between the *total* chemical potentials (μ_i) of the matter's constituents. The condition of equilibrium for the nuclear and Coulomb forces gives expressions for the chemical potentials of nuclei in terms of the chemical potentials of the free nucleons: $\mu_{A,Z} = Z\mu_{1,1} + (A - Z)\mu_{1,0}$. Equilibrium of the weak forces yields the beta reaction condition: $\mu_{1,1} + \mu_e = \mu_{1,0} + \mu_\nu$. In terms of the zeroth order chemical potentials, the beta equilibrium condition is

$$\mu_e^0 - \mu_\nu^0 = \mu_{1,0}^0 - \mu_{1,1}^0 - Q_1 - \frac{\partial}{\partial X_e}\left\langle \frac{Q}{A} \right\rangle + \frac{\partial}{\partial X_{1,0}}\left\langle \frac{B}{A} \right\rangle - \frac{\partial}{\partial X_{1,1}}\left\langle \frac{B}{A} \right\rangle . \tag{13}$$

Most hydrodynamics calculations (Arnett 1977; Wilson 1977; Mazurek 1979) use the Boltzmann expression for the nonleptonic chemical potentials with modified nuclear binding energies. It is instructive to write the condition for equilibria of the Coulomb and nuclear forces in such a form. The effects of nucleon degeneracy, Coulomb lattice energies, and nuclear interactions then appear as modifications to a nuclear binding energy. Explicitly,

$$\mu_{A,Z} = Z\mu_{1,1}^{\rm B} + (A - Z)\mu_{1,0}^{\rm B} + \Delta_{A,Z} , \tag{14}$$

$$\Delta_{A,Z} = \Delta_{A,Z}^{\rm deg} + \Delta_{A,Z}^{\rm coul} + \Delta_{A,Z}^{\rm nuc} , \tag{15}$$

$$\Delta_{A,Z}^{\rm deg} = Z(\mu_{1,1}^0 - \mu_{1,1}^{\rm B}) + (A - Z)(\mu_{1,0}^0 - \mu_{1,0}^{\rm B}) , \tag{16}$$

$$\Delta_{A,Z}^{\rm Coul} = ZQ_1 - Q_Z , \tag{17}$$

$$\Delta_{A,Z}^{\rm nuc} = -B_{A,Z} + Z\frac{\partial}{\partial X_{1,1}}\left\langle \frac{B}{A} \right\rangle + (A - Z)\frac{\partial}{\partial X_{1,0}}\left\langle \frac{B}{A} \right\rangle , \tag{18}$$

where $B_{1,1} = B_{1,0} = W$ completes the definition of $\langle B/A \rangle$, and $\mu^{\rm B}$ denotes Boltzmann chemical potentials. When exponentiated, equation (14) has the appearance of the usual nuclear Saha equation (cf., e.g., Burbidge *et al.* 1957)

$$n_{A,Z} = \Omega_{A,Z} A^{3/2} \left[\frac{h^2 N_0}{2\pi k_B T}\right]^{3/2(A-1)} \frac{n_{1,1}^{\ Z} n_{1,0}^{\ A-Z}}{2^A} \exp\left(\frac{\Delta_{A,Z}}{k_B T}\right) . \tag{19}$$

Note that $-\Delta_{A,Z}$ does not represent the binding energy of the nucleus. The reason for this is that the total energy per ion ($\frac{3}{2}k_B T + B_{A,Z}$) and the chemical potential with interaction ($\mu_{A,Z}^{\ B} - \Delta_{A,Z}$) must satisfy the thermodynamic identity

$$\frac{\partial}{\partial n_{A,Z}}[n_{A,Z}(\tfrac{3}{2}k_B T + B_{A,Z})]_T = -T^2 \frac{\partial}{\partial T}\left[\frac{\mu_{A,Z}^{\ B} - \Delta_{A,Z}}{T}\right]_{n_{A,Z}} , \tag{20}$$

where $B_{A,Z}$ is the binding energy. From equation (10) it can be seen that the kinetic contributions cancel and $B_{A,Z}$ satisfies

$$B_{A,Z} = T^2 \frac{\partial}{\partial T}\left(\frac{\Delta_{A,Z}}{T}\right) - n_{A,Z}\frac{\partial B_{A,Z}}{\partial n_{A,Z}} . \tag{21}$$

Therefore $-\Delta_{A,Z}$ equals the nuclear binding energy only if both $\Delta_{A,Z}$ and $B_{A,Z}$ are constant. In the present instance this is not the case, and solutions with $-\Delta_{A,Z}$ greater than zero that have nuclei present do exist.

f) *Solution Procedure*

An equilibrium network of 155 nuclei was used to solve for the equilibrium composition. The component nuclei of this network were chosen so as to give maximal representation around regions where the abundances peaked. These peaks generally occur in regions far from the valley of beta stability. Hence the binding energies of these nuclei have not been measured experimentally. We adopted Mackie's (1976) mass formula to derive the relevant binding energies. For the nuclei under consideration, his results generally agree to within 5% with those

of Garvey *et al.* (1969). For fixed X_e and $\Delta_{A,Z}$'s the equilibrium composition can be obtained through well known procedures (cf., e.g., Clifford and Taylor 1964). Generally the composition obtained gives a different $\Delta_{A,Z}$ from the one initially used, so iteration must be used until a consistent solution is found. Once this is done, the neutrino chemical potential, and hence the total lepton number, is given by the beta equilibrium condition of equation (13).

III. DISCUSSION

This section examines the relative importance of nucleon degeneracy, Coulomb lattice energy, nuclear interactions, and partition functions in the dissociation of the heavy nuclei. We first give numerical expressions for the various effects. The relative importance of each can be estimated in the context of the Saha equation (19). In magnitude the Coulomb interaction energy is a small fraction of the corrections to the effective nuclear binding energies introduced by nucleon degeneracy and nuclear interactions. The nuclear partition functions play a significant role in preventing nuclear dissociation until the densities become sufficiently high for nuclear forces to become important. The condition that one-half of the mass be in the form of free nucleons is used to define dissociation curves that result from the various processes discussed. The dissociation curves seem to level off with increasing densities at around $k_BT \approx 10$ MeV when all of the physical processes are included.

a) Magnitudes of the Different Effects

i) *Nucleon Degeneracy*

The differences of the chemical potentials in equation (16) were computed using numerical techniques accurate to 0.1%. Cruder but analytic approximations for these quantities are possible. In particular, they can be expressed as unique functions of the Boltzmann chemical potential of equation (10), which can be written numerically for nucleons as

$$\eta_n{}^B = 2.76 + \ln X_n\rho_{13} - \tfrac{3}{2}\ln T_{10}\,, \tag{22}$$

where η represents the ratio of chemical potential to k_BT, n denotes either neutrons or protons, $\rho_{13} = \rho/10^{13}$ g cm^{-3}, and $T_{10} = T/10^{10}$ K. For a given η the logarithm of the right side of equation (11) gives η^B. Figure 1 shows $\log(\eta - \eta^B)$ as a function of η^B. The relation is nearly linear for $\eta^B < 2.5$. For $\eta^B > 2.5$ the gas is sufficiently degenerate that the zero-temperature approximation to the Fermi integral in equation (11) gives reasonable results. Combining the results of Figure 1 with equation (22) for low degeneracy, and using the zero-temperature approximation otherwise, gives

$$\frac{\mu_n{}^0 - \mu_n{}^B}{\text{MeV}} = 4.26(X_n\rho_{13})^{0.962}T_{10}{}^{-0.444}\,, \qquad \text{for } \eta_n{}^B \le 2.5$$

$$= 0.862T_{10}\left\{\left[\frac{3\pi^{1/2}}{4}\exp(\eta_n{}^B)\right]^{2/3} - \eta_n{}^B\right\}, \quad \text{otherwise}\,. \tag{23}$$

This expression is accurate to within 5% for all $\eta_n{}^B$.

ii) *Nuclear Partition Functions*

We have adopted the semiempirical level density formulae of Gilbert and Cameron (1965) to determine nuclear partition functions. The increase in the partition functions has dramatic effects on the composition of the matter

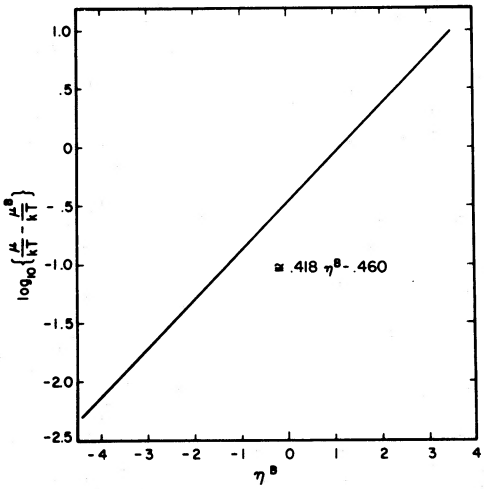

FIG. 1.—The difference between Fermi and Boltzmann chemical potentials as a function of the latter (in units of k_BT)

for temperatures greater than $kT \approx 3$ MeV. A representative nucleus of those that dominate the composition in the results below is ^{40}P. Using the approximations given in the Appendix, its partition function is ($a_{40,15} = 7.46$/MeV)

$$\ln \Omega_{40,15} \cong -1.82 + 6.43T_{10} + \ln q[(6.43T_{10})^{1/2}] - \tfrac{1}{2} \ln T_{10}\,, \tag{24}$$

where the functional form of $q(x)$ is given in the Appendix and its dependence on x is plotted in Figure 2. The mean excitation energy is given by

$$\langle E \rangle / \text{MeV} \approx 0.431 T_{10} q^{-1}[(6.43T_{10})^{1/2}]\,. \tag{25}$$

Equation (24) agrees with the numerical calculations of ln Ω to within 5%. Equation (25) shows that the mean excitation energy increases rapidly with temperature, and for $T_{10} \geq 7.5$ it becomes greater than the binding energy. For such temperatures our assumption of Boltzmann nuclei with internal excitations breaks down. The free energy of the system of interacting nucleons in general will differ when the average energy of a single nucleon within the system is of the order of its separation energy. The approach used to derive the nuclear partition functions must be modified.

The basic problem arises from the fact that some fraction of the very excited nuclear states contains single particles in the continuum, and a residual nucleus. Therefore the possibility exists that the multiplicity of such configurations may be overestimated if they are not removed from the partition functions of individual nuclei (Fowler, Engebrecht, and Woosley 1978). Note that typically many nuclei share the total excitation energy (Bethe 1937). Thus there will in general be many more states without particles in the continuum. At an excitation energy of ~16 MeV and for nuclear separation energies of ~8 MeV, Steve Koonin (Caltech, private communication) estimates that the fraction of levels with a single particle excited above its separation energy is $\lesssim 0.07$. Our own estimates in the Appendix indicate that this fraction is very sensitive to the particle separation energies. For the neutron-rich nuclei, it can approach unity at excitation energies in the range 15–25 MeV.

Of the states with particles in the continuum, the sharp resonances should be counted as bound states. Calculations of nuclear partition functions with continuum single particle states subtracted out and sharp resonance states included are presented by Fowler *et al.* Their results show partition functions leveling off and becoming constant at average excitation energies ~10–13 MeV. Such results indicate that the nonresonant levels with particles in the continuum contribute appreciably to the total level density. However, Fowler *et al.* dealt with nuclei whose nucleon separation energies are $\gtrsim 8$ MeV. Our Table 2 in the Appendix shows that the fraction of *all* levels with particles above separation energies is below 0.1. Therefore we believe that the procedure used by these authors overestimates by a considerable amount the number of continuum single particle states that need to be subtracted out.

The contribution from the sharp resonances which should be included in the partition functions is expected to be large (A. K. Kerman, MIT, private communication). Furthermore, putting n particles in m bound levels must necessarily give a Gaussian distribution, centered at half the binding energy of the nucleus. Therefore, one expects that the Fermi gas formula for nuclear level densities is valid at all energies that are small in comparison to the latter quantity, which is around 200–250 MeV.

In the numerical calculations below, we have included only levels below 25 MeV. This cutoff in the partition functions is meant to approximate the subtraction of *nonresonant* levels with particles in the continuum. For the neutron-rich nuclei of interest, the fraction of *all* nuclear levels with continuum single particles can be large (cf.

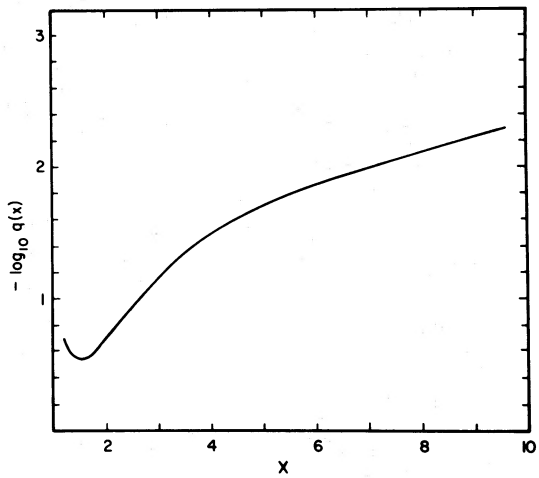

FIG. 2.—The mean excitation energy of a nucleus as a function of $(a_{A,Z}k_BT)^{1/2}$ (in units of $k_BT/2$)

Appendix). However, as noted above, many such levels are sharp resonances and should be included in the partition function. Because of this, we feel that the procedure with a 25 MeV cutoff probably underestimates the actual partition functions.

iii) *Nuclear Interaction Energies*

Equation (18) may be written in the form

$$\Delta_{A,Z}^{\rm nuc} = -B_{A,Z}^{0} + AW + (X_{1,1} + X_{1,0})\left[Z\,\frac{\partial W}{\partial X_{1,1}} + (A - Z)\frac{\partial W}{\partial X_{1,0}}\right] + \left[-\chi_{A,Z} + Z\sum_{A',Z'>1}\frac{X_{A',Z'}}{A'}\frac{\partial \chi_{A',Z'}}{\partial X_{1,1}} + (A - Z)\sum_{A',Z'>1}\frac{X_{A',Z'}}{A'}\frac{\partial \chi_{A',Z'}}{\partial X_{1,0}}\right], \quad (26)$$

where $B_{A,Z}^{0}$ is the binding energy of the nucleus in vacuum, and $\chi_{A,Z} = B_{A,Z} - B_{A,Z}^{0}$. The terms in the last brackets represent the effects of the changes in binding energies of nuclei due to the interactions with the free nucleons. These terms could be determined by solving the pressure balance equation across the nuclear surface (eq. [2.6] in Mackie 1976). However, the complexity of such an approach makes it impractical when dealing with a network of over 100 nuclei. For simplicity we neglect this term in our numerical calculations below. The remaining expression for the nuclear binding energy after some rearrangement is

$$\Delta_{A,Z}^{\rm nuc} = -B_{A,Z}^{0} + AW + \{Z - A\beta\}\left(\frac{\partial W}{\partial \beta}\right)_{k} + A(X_{1,1} + X_{1,0})\left(\frac{\partial W}{\partial X_{n}}\right)_{\beta}. \quad (27)$$

Table 1 gives W and its relevant derivatives for typical values of $(X_{1,1} + X_{1,0})\rho$ and β.

For the purposes of the discussions below, this neglect of binding energy variations can be justified. The change in total binding energy in the presence of external nucleons is due to modifications in the Coulomb and surface energies of the nucleus. In a sea of free nucleons, the surface energy is decreased from its value in vacuum by the factor

$$\left(1 - \frac{W}{W_{\rm nuc}}\right)^{1/2}\left[1 - (X_{1,1} + X_{1,0})\,\frac{\rho}{\rho_{\rm nuc}}\right]^{4/3},$$

where $W_{\rm nuc}$ and $\rho_{\rm nuc}$ are the bulk energy and the matter density inside the nucleus (cf. eq. [4.15] in Mackie 1976). The latter have typical values of $W_{\rm nuc} \approx 16$ MeV and $\rho_{\rm nuc} \approx 2 \times 10^{14}$ g cm^{-3}. Thus at low densities ($\rho \lesssim 2 \times 10^{13}$ g cm^{-3}) the decrease in the surface energy is represented by a factor between 0.85 and unity for $X_{1,1} + X_{1,0} \leq 0.5$. In addition, the density of external charged particles is low and the Coulomb energy does not change appreciably. Therefore, the change in the total binding energy is less than 15% at low densities. For high densities ($\rho \gtrsim 2 \times 10^{13}$ g cm^{-3}) it is necessary to distinguish between cold and hot matter. For hot ($kT \gtrsim 8$ MeV) matter, the effects of nuclear partition functions determine the nuclei in equilibrium (cf. § III below). Since the influence of the nuclear binding energies is dramatically diminished, so are the effects of changes in Coulomb and surface energies. Such effects were studied by Lamb *et al.* (1979). They find that dissociation curves like those discussed below are relatively insensitive to changes in Coulomb and surface energies. On the other hand, for high densities and low temperatures, the influence of excited nuclear states diminishes. For sufficiently low temperatures, dramatic differences in the characteristics of the nuclei in equilibrium can result from differences in the

TABLE 1

TYPICAL VALUES OF THE FREE-NUCLEON INTERACTION ENERGY AND ITS DERIVATIVES (in MeV)

$(X_{1,1} + X_{1,0})\rho$	$-W(k,\beta)$			$-(\partial W/\partial X_n)_\beta$			$-(\partial W/\partial\beta)_k$		
5.000E+12*	1.066	1.206	1.314	1.105	1.219	1.293	1.986	1.109	1.073
1.000E+13	2.114	2.382	2.572	1.998	2.277	2.451	3.844	2.049	1.789
1.500E+13	3.076	3.490	3.770	2.788	3.241	3.519	5.795	3.155	2.515
2.000E+13	3.978	4.546	4.921	3.508	4.133	4.515	7.775	4.343	3.244
3.000E+13	5.649	6.534	7.102	4.790	5.746	6.330	11.717	6.824	4.689
4.000E+13	7.184	8.386	9.148	5.910	7.171	7.943	15.566	9.341	6.104
5.000E+13	8.611	10.125	11.078	6.901	8.438	9.383	19.286	11.834	7.479
6.000E+13	9.949	11.765	12.905	7.781	9.567	10.668	22.859	14.271	8.810
7.000E+13	11.208	13.317	14.637	8.565	10.570	11.812	26.278	16.635	10.096
8.000E+13	12.398	14.788	16.282	9.262	11.458	12.825	29.540	18.915	11.335
9.000E+13	13.525	16.183	17.845	9.880	12.239	13.715	32.643	21.105	12.526
1.000E+14	14.595	17.509	19.331	10.424	12.919	13.490	35.588	23.201	14.671
β =	0.1	0.2	0.3	0.1	0.2	0.3	0.1	0.2	0.3

* Numbers following E denote powers of 10.

functional form of the surface energy (cf. the review of zero-temperature results by Canuto 1974). The dissociation curves presented below are hot at high densities. Our neglect of the Coulomb and surface modifications is in this sense justified.

iv) *Coulomb Lattice Energy*

The numerical forms of equations (1) and (17) are

$$\Gamma_Z(a_Z k_B T) = 0.490 Z^{5/3}(X_e \rho_{13})^{1/3} T_{10}^{-1}, \tag{28}$$

and

$$\Delta_{A,Z\mathrm{Coul}}/\mathrm{MeV} = -0.380(X_e\rho_{13})^{1/3}\left\{Z^{5/3}\left[1 + \frac{4}{\Gamma_Z(a_Z k_B T)}\right]^{-1/2} - Z\left[1 + \frac{4}{\Gamma_Z(a_Z k_B T)}\right]^{-1/2}\right\}. \tag{29}$$

Thus Coulomb lattice energies are typically much below degeneracy energies if $X_n \approx X_e$. This is the case for neutrons, and we use only the simple version of equation (29) with $T = 0$ in the numerical calculations below.

b) Dissociation Curves

To estimate the relative importance of each process above, we compute dissociation curves for a value of the total lepton number that is typically obtained in current hydrodynamic calculations ($X_e + X_\nu \approx 0.33$). Three cases are considered. In the first, the nucleons as well as the nuclei are treated like Boltzmann particles and only the ground-state spins are used for the nuclear partition functions. The second case uses the nuclear partition functions with the Gilbert and Cameron (1965) level densities and a 25 MeV cutoff; the other assumptions of case one are retained. Finally in the third case we treat the nucleons as Fermi particles, use the partition functions of case (2) for the nuclei, and include the nuclear and Coulomb interaction energies discussed above.

i) *The Effects of Partition Functions*

Figure 3 compares the results of the first two cases where the nucleons as well as the nuclei are treated as Boltzmann particles. The curves give the line in the (ρ, T)-plane along which the composition of the matter consists of 50% free nucleons with the remainder being in the form of heavier elements. The open circles show the path followed by the central region in Mazurek's (1979) hydrodynamic calculations. His equation of state corresponds to case (2) above. The figure indicates that for $\rho_{13} \lesssim 0.1$ there is essentially no difference between the two dissociation curves, and the effects of the partition functions on the dissociation of the heavy nuclei are negligible. The importance of partition functions increases steadily for the higher dissociation temperatures at greater densities. For $\rho_{13} \gtrsim 1$ there is a considerable difference between the two dissociation curves. The path of the central zone in the hydrodynamic calculations seems to follow the dissociation curve at low densities. When the effects of the

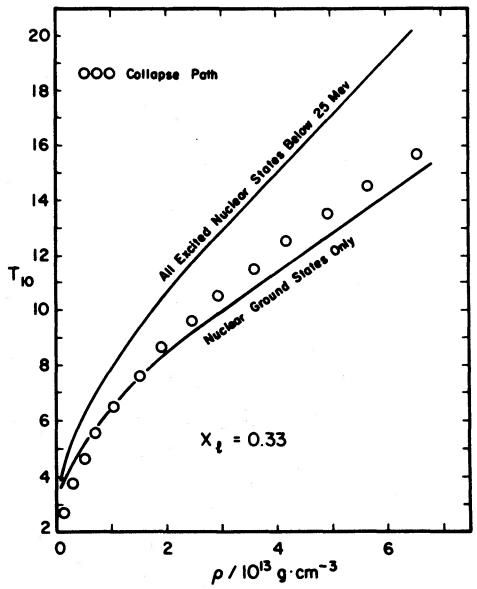

FIG. 3.—The effects of partition functions on nuclear dissociation. The curves are defined by the requirement that 50% of the matter be in the form of free nucleons. The path followed by the central region in Mazurek's (1979) hydrodynamic calculations is also shown. The dynamic calculations used an equation of state corresponding to the upper solid line.

partition functions become important, the path drops below the dissociation curve, indicating that the compressional heating is not sufficient to dissociate the matter.

The partition functions increase rapidly and at high temperatures become more important than the binding energies in determining the predominant species in equilibrium. This can be seen by writing equation (14) in the form

$$\frac{(\mu_{A,Z}{}^{B})^{\Omega=1}}{k_B T} = \frac{Z}{A}\frac{\mu_{1,1}{}^{B}}{k_B T} + \left(1 - \frac{Z}{A}\right)\frac{\mu_{1,0}{}^{B}}{k_B T} + \frac{B_{A,Z}}{Ak_B T} + \frac{\ln \Omega_{A,Z}}{A}, \tag{30}$$

where the partition function has been factored out explicitly. At high temperatures $A^{-1} \ln \Omega_{A,Z} \rightarrow a_{A,Z} k_B T/A$, becoming comparable to $B_{A,Z}/Ak_B T$. Thus the nuclei that dominate the composition are those that have the greatest $a_{A,Z}/A$. In the Gilbert and Cameron (1965) formulation the latter quantity is a linear function of the sum of the shell corrections for the neutrons and the protons. For $Z < 50$ their Table 3 indicates that the sum is greatest for $Z \approx 12$ and $(A - Z) \approx 23$. Therefore nuclei with $A \approx 35$–40 dominate the composition in our calculations. Note that no particular species is predominant. Rather, the composition clusters around these values of A and Z, with several tens of different nuclei being present.

ii) *The Effects of Nuclear Forces*

Figure 4 compares the dissociation curve for the case of Boltzmann nuclei with partition functions and Boltzmann nucleons to that of the case which also includes the Fermi behavior of the nucleons, the Coulomb lattice energy, and the nuclear interactions between nucleons. Again, both curves merge for densities below 10^{12} g cm^{-3}. The nuclear forces induce dissociation at lower temperatures for densities above 10^{13} g cm^{-3}. The path followed in the collapse calculation crosses the latter curve at $\rho_{13} \approx 2$. Thus a calculation of collapse with nuclear forces included will lead to greater dissociation, and hence to a cooler collapse path. The pressure contribution of the free nucleons will be lower, and the core can be expected to bounce at greater densities.

A rather significant aspect of the nuclear forces between nucleons that has not been taken into account in the current hydrodynamic calculations is the concomitant pressure reduction. For a Boltzmann gas of free nucleons the pressure reduction is given by the factor

$$p_{\rm int}/p = 1 - \frac{X_n}{k_B T}\left(\frac{\partial W}{\partial X_n}\right)_{\beta}, \tag{31}$$

where p represents the pressure. This factor is plotted in Figure 5. Note that for densities where the nuclear forces enhance dissociation, the free nucleon pressure contribution is reduced significantly. This effect also serves to shift the bounce toward higher densities.

c) Summary

The shifts in dissociation curves with variations in input physics are large for $\rho_{13} \gtrsim 2$. These large shifts indicate that at higher densities the uncertain physics will have dramatic effects on the equation of state for stellar collapse

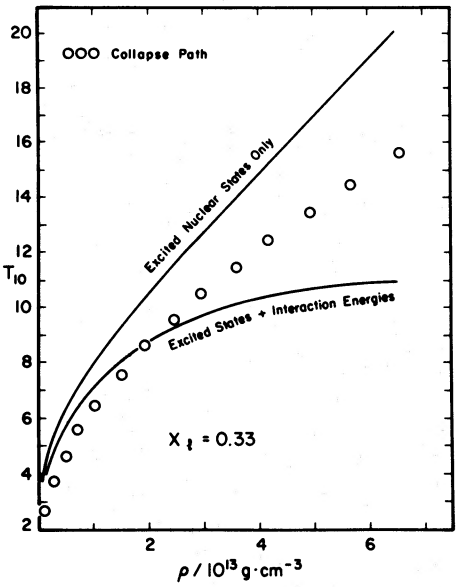

FIG. 4.—The solid lower line is the dissociation curve which includes the effects of nuclear and coulomb interaction energies, partition functions, and nucleon degeneracy. The legend to Fig. 3 describes the other features shown.

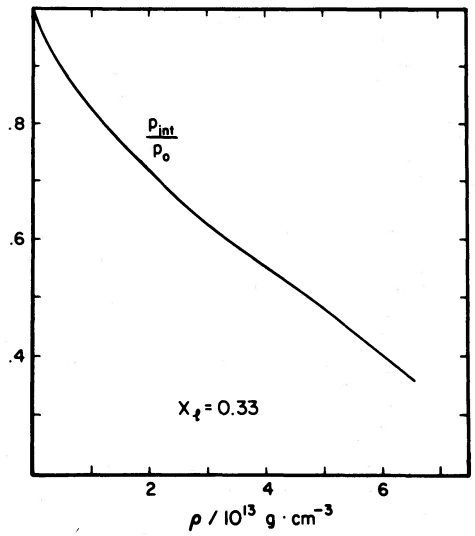

FIG. 5.—The ratio of the free-nucleon pressure with nuclear interaction to that without along the lower dissociation curve of Fig. 4 (cf. eq. [36]).

work. The effects of this partial degeneracy of the free neutrons and the large partition functions of nuclei act to preserve the nuclei. Nuclear interaction between the free nucleons enhances dissociation. The effects of the Coulomb lattice energy are negligible. The interaction between free nucleons also decreases their pressure contribution. The greatest uncertainties in how the combination of these effects determines the equation of state lie at densities greater than $\rho_{13} \gtrsim 1$. At densities below this, the above effects are small along the dissociation curve. The usual nuclear Saha equation with vacuum binding energies for the nuclei may be used to determine the composition of the lower densities.

The dissociation curve with all processes included initially increases with increasing densities. It then levels off toward a limiting value of $T_{10} \approx 11$, for $\rho_{13} \gtrsim 5$. This limiting temperature is roughly half the value obtained by Lattimer and Ravenhall (1978, their Fig. 5 with T_c evaluated at $X_d \approx 0.2$). Generally their dissociation curves lie closer to the top curve of our Figure 4. The reasons for this discrepancy are not readily apparent since the two approaches differ radically. One possible way that our results could be brought into closer agreement with theirs is through the neglect of our 25 MeV cutoff in the partition functions of the nuclei. The rapid increase in partition functions at the greater dissociation temperatures of higher densities would then tend to act counter to the effects of nuclear binding between free nucleons. Partition functions do not enter explicitly into the formalism of Lattimer and Ravenhall, and it is difficult to determine if this is indeed the problem. Further work will be required to determine the source of the discrepancy.

Improvements in the input physics may change some of the details of our results. However, the importance of nuclear partition functions and nuclear interaction between free nucleons in determining the dissociation of the nuclei is clearly demonstrated by Figures 3 and 4. These effects become significant for $\rho_{13} \gtrsim 1$. In all of the dynamic calculations to date the core bounces at central densities above this value. The uncertainties in the input physics at these higher densities make the equation of state uncertain. Hence the results regarding the outcome of collapse are questionable.

A comparison of the results of various dynamic calculations is shown in Figure 6. The temperature-density behavior of the central region during collapse that has been obtained in recent work is shown. All of the calculations agree for $\rho_{13} \lesssim 0.01$. Since each calculation used a different initial model, the agreement indicates that the thermal behavior of the core is determined by the nuclear dissociation. Compressional energy is used up in dissociating heavy nuclei and in providing the $3k_BT/2$ of kinetic energy acquired by each nucleon that is freed. The core thus evolves near the dissociation curve. At these lower densities the input physics is well determined so that very similar results are obtained by the various researchers.

As ρ_{13} exceeds 0.1, discrepancies between the different results become pronounced. These discrepancies are probably due to differences in input physics. The results of Bruenn, Arnett, and Schramm (1977) show a markedly hotter collapse due to their neglect of the degeneracy of the neutrinos. A hotter collapse is obtained without neutrino degeneracy because all of the energy of the degenerate electrons is converted to heat. When the leptonic nature of neutrinos is taken into account, neutrino trapping and degeneracy results. This means that most of the energy of the electrons remains as zero-point energy of both electrons and neutrinos. Therefore, less energy is available for heating.

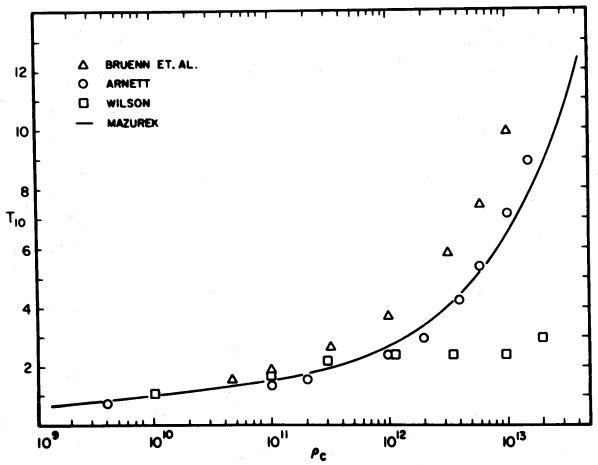

FIG. 6.—The temperature and density in the center of the stellar core during collapse. The results shown are those of Arnett (1977), Bruenn *et al.* (1977), Wilson (1977), and Mazurek (1979).

The results of Arnett (1977) and Mazurek (1979) essentially agree up to the point where Arnett's calculation stops ($\rho_{13} \approx 1.5$). Mazurek's calculations included the effects of nuclear partition functions while Arnett's did not. No differences in results appear, however, since the partition functions become important only at higher densities.

Wilson's (1977) results deviate significantly from those of the other calculations for $\rho_{13} \gtrsim 0.4$. His equation of state includes the effects of nuclear forces. Therefore, he obtains total dissociation of the nuclei at lower densities. The absorption of thermal energy by dissociation results in a cooler collapse. However, Wilson's results indicate total dissociation even below the highest density point shown in Figure 6. Since $T_{10} \lesssim 3$ throughout his stellar core, this is at variance with our results. Figure 4 indicates that his central conditions fall considerably below our dissociation curve.

The different equations of state used in collapse calculations give definite differences in the thermal behavior of the core. These differences in thermal behavior probably account for the different outcomes obtained by the calculations of Wilson (explosion) and of Mazurek (total collapse). A better understanding of the equation of state at the higher densities is needed to determine the outcome of stellar collapse. Specific areas that require further work include (*a*) finite temperature effects on the free energy arising from nuclear forces; (*b*) the effects of the free nucleons on the binding energy of the nuclei; and (*c*) the behavior of nuclear partition functions at high temperatures.

We are thankful to H. A. Bethe and D. Q. Lamb for useful discussions, and gladly acknowledge the hospitality of the Aspen Center for Physics where some of this work was completed.

APPENDIX

a) The Binding Energy of the Free Nucleons

For completeness, we quote from Baym, Bethe, and Pethick (1971) the functional form of the bulk binding energy that was used in our calculations. The interested reader is referred to that work for more details. The expression is

$$W(k,\beta) = \left[W(k,\tfrac{1}{2}) - \frac{3\hbar^2k^2N_0}{10}\right](1 - 3\alpha^4 + 2\alpha^6) + \left[s\left(\frac{k}{k_0}\right)^2 - \frac{\hbar^2k^2N_0}{6}\right]\alpha^2(1-a^2)^2$$
$$+ \left[W(k,0) - \frac{2^{2/3}3}{10}\hbar^2k^2N_0\right](3\alpha^4 - 2\alpha^6) + \left[\mu_p^{(0)} - \mu_n^{(0)} + 2^{2/3}\frac{\hbar^2k^2N_0}{2}\right]\frac{(\alpha^4 - \alpha^6)}{4}, \quad \text{(A1)}$$

where $\alpha = 1 - 2\beta$, $\hbar = h/2\pi$, and

$$W(k,\tfrac{1}{2}) = 0.3\hbar^2k^2N_0\left(1 - \frac{k}{k_0}\right)^3 - W_0\left(\frac{k}{k_0}\right)^3\left[1 + \left(1 - \frac{k}{k_0}\right)\left(9 - 6\frac{k}{k_0}\right)\right] + \tfrac{1}{2}K\left(1 - \frac{k}{k_0}\right)^2\left(\frac{k}{k_0}\right)^3. \quad \text{(A2)}$$

To complete the specification of $W(k, \beta)$, we have used Mackie's (1976) expressions for

$$W(k, 0) = 1.30k + 15.0k^2 - 15.2k^3 + 7.47k^4 , \tag{A3}$$

and

$$\mu_p^{(0)} = 23.2k - 142.k^2 + 38.7k^3 + 7.12k^4 , \tag{A4}$$

where $W(k, 0)$ and $\mu_p^{(0)}$ are in MeV, k is in fm^{-1}, and the remaining constants are: $k_0 = 1.34\ \mathrm{fm}^{-1}$; $W_0 = 15.5$ MeV; $s = 27.1$ MeV; $K = 268$ MeV.

The remaining parameter is given by

$$\mu_n^{(0)} = W(k, 0) + \tfrac{1}{3}k \frac{\partial W(k, 0)}{\partial k} . \tag{A5}$$

Note that our $W(k, \beta)$ of equation (A1) omits the zero-temperature kinetic energy.

b) The Nuclear Partition Functions at High Temperatures

In the numerical results presented in § III, we have used the procedure given by Gilbert and Cameron (1965) to define the level density of excited states. This level density was integrated numerically to obtain the nuclear partition function. The level density has two functional forms which are joined smoothly at some transition energy. At low energies, the level density has an exponential form $\omega(E)\alpha \exp(E/\tau)$, where $\omega(E)$ is the level density (number per MeV) at excitation energy E, and τ is the "nuclear temperature." This form holds up to excitation energy E_x. They define a new variable U by subtracting pairing energies from the excitation energy. In terms of this variable the transition from the simple exponential form to a more complex expression occurs at

$$U_x = E_x - E_Z^p - E_{A-Z}^p = (2.5 + 150A^{-1})\ \mathrm{MeV} , \tag{A6}$$

where E_Z^p and E_{A-Z}^p represent the pairing energies in their model of the protons and neutrons, respectively. Above this energy, a level density based on the Fermi gas model (Bethe 1937) is used. The latter may be expressed as

$$\omega(U) = C \frac{\exp(4aU)^{1/2}}{(4aU)^{3/2}} ; \qquad C = \frac{2}{3(0.1777)^{1/2}} \frac{a}{A^{1/3}} , \tag{A7}$$

where a/A depends linearly on the sum of the two shell corrections

$$a/A = [0.00917(E_Z^S + E_{A-Z}^S) + (a/A)_0]\ \mathrm{MeV}^{-1} \tag{A8}$$

with $(a/A)_0$ equaling 0.142 and 0.120 for undeformed and deformed nuclei, respectively. For Z below 30 the deformed nuclei are taken to be those with $20 \leq Z \leq 30$, and the undeformed ones are those with $Z \leq 20$. For heavier nuclei, the deformed ones are those which have Z or $A - Z$ more than 3 units away from a magic number.

At the high temperatures of interest the partition function is dominated by the levels at high energies above E_x. Thus the partition function is approximately given by

$$\Omega_{A,Z} \approx \int_{U_x}^{\infty} \exp\left(-\frac{E}{k_B T}\right) \omega(U) dU = \frac{C \exp[(E_Z^p + E_{A-Z}^p)/k_B T]}{(4a)^{3/2}(k_B T)^{1/2}} I_0\left[\frac{U_x}{k_B T}, (4ak_B T)^{1/2}\right] , \tag{A9}$$

where

$$I_0(x_0, \alpha) = \int_{x_0}^{\infty} \exp(-x + \alpha x^{1/2}) x^{-3/2} dx .$$

We now derive a useful approximation to the partition function at high temperatures. Integration by parts yields

$$I_0(x_0, \alpha) = 2{x_0}^{-1/2} \exp(-x_0 + \alpha {x_0}^{1/2}) + \alpha \int_{x_0}^{\infty} \frac{\exp(-x + \alpha x^{1/2})}{x} dx - 2I_1(x_0, \alpha) , \tag{A10}$$

where

$$I_1(x_0, \alpha) = \int_{x_0}^{\infty} \frac{\exp(-x + \alpha x^{1/2})}{x^{1/2}} dx = 2 \exp(\alpha^2/4) \int_{{x_0}^{1/2} - \alpha/2}^{\infty} \exp(-x^2) dx . \tag{A11}$$

The explicit integral in equation (A10) satisfies

$$\frac{d}{d\alpha} \int_{x_0}^{\infty} \frac{\exp(-x + \alpha x^{1/2})}{x} dx = I_1(x_0, \alpha) . \tag{A12}$$

In the limit $\alpha/2 - x_0^{1/2} \gg 1$, equation (A12) can be integrated to yield

$$\lim_{(\alpha/2 - x^{1/2}) \to \infty} \int_{x_0}^{\infty} \frac{\exp(-x + \alpha x^{1/2})}{x} dx = 2\pi^{1/2} \int_0^{\alpha} \exp(\tfrac{1}{4}x^2) dx + \int_0^{\infty} \frac{e^{-x}}{x} dx . \quad \text{(A13)}$$

Over the range of interest $x_0 \approx 1$, so that the last term in equation (A13) and the first term on the right side of equation (A10) are negligible. In this limit the partition function is given by

$$\Omega_{A,Z} \approx \frac{C \exp[(E_Z{}^p + E_{A-Z}{}^p)/k_B T]}{(4a)^{3/2}(k_B T)^{1/2}} \{4\pi^{1/2} \exp(ak_B T) q[(ak_B T)^{1/2}]\} , \quad \text{(A14)}$$

where

$$q(\alpha) = 2\alpha \exp(-\alpha^2) \int_0^{\alpha} \exp(x^2) dx - 1 , \quad \text{(A15)}$$

and can be evaluated from the tables given by Karpov (1965). The mean excitation energy of the nucleus is given by

$$\langle E \rangle = \Omega_{A,Z}{}^{-1} \left\{ \frac{C \exp[(E_Z{}^p + E_{A-Z}{}^p)/k_B T](k_B T)^{1/2}}{(4a)^{3/2}} I_1 \left[\frac{U_x}{k_B T}, (4ak_B T)^{1/2} \right] \right\} = \frac{k_B T}{2} q^{-1}[(\alpha k_B T)^{1/2}] , \quad \text{(A16)}$$

where in the integration we have set $E = U$.

Note that in the main text $a_{A,Z}$ is used for a to distinguish it from the symbol for the ion-sphere radius a_Z.

c) Fractions of Nuclear States with Single Particles Excited above Separation Energies

We now estimate the fraction of the total nuclear levels below a given excitation energy that have particles excited above separation energies. Such levels will become significant only at higher excitation energies, and hence the level density will be that of equation (A7). We consider only the states with either one or two particles having energies in excess of that required for separation, and deal with neutrons and protons separately. For the purposes of this rough estimate of such levels, we assume that the variable a in equation (A8) is constant over the nuclear species that dominate the composition, with $a = 7\ \mathrm{MeV}^{-1}$. The level densities depend only mildly on A. The nuclei that dominate the composition (cf. discussion in § III) fall in the range $35 \lesssim A \lesssim 40$, and negligible error is introduced by keeping a constant.

First consider the levels with a single particle excited above its separation energy. The excitation energy in such configurations is shared between the particle and the residual nucleus. For a fixed excitation energy of the residual nucleus, E_{A-1}, the particle's energy has a fixed value, and the multiplicity of levels is just a product of the number of directions that the particle can have and its spin multiplicity. The total number of such levels is then an integral over the possible level densities of the residual nucleus times the constant single particle multiplicity of levels. Explicitly,

$$\Lambda_1(E_A, E_{\min}) = 8\pi \int_{E_{\min}}^{E_A - \Delta_n{}^A} \omega(E_{A-1}) dE_{A-1} = \frac{2\pi C}{a} \int_{4aE_{\min}}^{4a(E_A - \Delta_n{}^A)} \frac{\exp(x^{1/2}) dx}{x^{3/2}} , \quad \text{(A17)}$$

where $\Lambda_1(E_A, E_{\min})$ is the total number of levels with a single particle above its separation energy for excitation energies below E_A in the nucleus with mass number A, $E_{\min}$ is the minimum energy where equation (A7) is valid, $\Delta_n{}^A$ is the separation energy of the particle, and the subscript denotes either neutrons or protons. The integral in equation (A17) can be transformed to give

$$\Lambda_1(E_A, E_0) = \frac{4\pi C}{a} \frac{e^{y_1}}{y_1{}^2} \int_0^{y_1 - y_{\min}} \frac{e^{-z} dz}{(1 - z/y)^2} \approx \frac{4\pi C}{a} \frac{e^{y_1}}{y_1{}^2} , \quad \text{(A18)}$$

where $y_1 = [4a(E_{A-1} - \Delta_n{}^A)]^{1/2}$ and $y_{\min} = (4aE_0)^{1/2}$. The rightmost expression in equation (A18) is accurate to better than 20% when $y \geq 12$ and $y_{\min} \leq 9$, which is adequate for our purposes.

Now consider the levels with two particles excited above their separation energies. For a given excitation energy of the residual nucleus, the two particles share the remaining energy. For a given energy of one of the particles, the energy of the second one is fixed and its level multiplicity is equal to that discussed above. The number of levels possible for the first particle is just equal to the total number of single particle levels below $E_A - \Delta_n{}^A - \Delta_n{}^{A-1} - E_{A-2}$, where $\Delta_n{}^{A-1}$ is the separation energy of the second particle and E_{A-2} is the excitation energy of the residual nucleus. An integral over the products of $\omega(E_{A-2})$ with the two single particle level multiplicities then yields an estimate of the number of levels with two particles above their separation energies. Explicitly,

$$\Lambda_2(E_A, E_{\min}) = 8\pi \left[\frac{1}{n_n{}^{\mathrm{nuc}}} \right] \frac{8\pi}{3h^3} \int_{E_{\min}}^{E_A - \Delta_n{}^A - \Delta_n{}^{A-1}} [2m_n(E_A - \Delta_n{}^A - \Delta_n{}^{A-1} - E_{A-2})]^{3/2} \omega(E_{A-2}) dE_{A-2} , \quad \text{(A19)}$$

TABLE 2

UPPER LIMIT δ_1^s ON THE FRACTIONS OF LEVELS WITH ONE PARTICLE EXCITED ABOVE ITS SEPARATION ENERGY FOR VARIOUS NUCLEAR EXCITATION AND PARTICLE SEPARATION ENERGIES ($a = 7$ MeV^{-1})

	E/MeV		
($\Delta_n{}^A$/MeV)	15	25	50
4.....	1.8	3.3	5.9
6.....	4.1 (−1)	1.1	2.8
8.....	8.1 (−2)	3.6 (−1)	1.3
10.....	1.3 (−2)	1.1 (−1)	6.0 (−1)
12.....	1.5 (−3)	3.0 (−2)	2.7 (−1)
14.....	9.4 (−5)	7.7 (−3)	1.2 (−1)
16.....	0	1.8 (−3)	5.2 (−2)

NOTE.—Numbers in parentheses denote powers of 10.

where m_n is the mass of a nucleon, and $n_n{}^{\rm nuc}$ is the density of either neutrons or protons in the nucleus. An upper limit is obtained by setting $E_{A-2} = 0$ in the square brackets of equation (A19). With the same approximation for the intergal as in equation (A17), one obtains

$$\Lambda_2(E_A, E_{\rm min}) \leq \frac{8\pi}{3}\left(\frac{1}{n_n{}^{\rm nuc}}\right)\left(\frac{m_n y_2{}^2}{2ah^2}\right)^{3/2}\left(\frac{4\pi C}{a}\frac{e^{y_2}}{y_2{}^2}\right), \tag{A20}$$

where $y_2 = [4a(E_A - \Delta_n{}^A - \Delta_n{}^{A-1})]^{1/2}$.

We now can compute upper limits to the fractions of nuclear levels with one and with two particles excited above their separation energies. The total number of levels below E_A is

$$\Lambda_0(E_A, E_{\rm min}) = \int_{E_{\rm min}}^{E_A} \omega(E)dE \approx \frac{C}{2a}\frac{e^{y_0}}{y_0{}^2}, \tag{A21}$$

where $y_0 = (4aE_A)^{1/2}$ and the previous integral approximation was used again. The fraction of levels with a single particle above its separation energy therefore satisfies

$$\frac{\Lambda_1}{\Lambda_0} \lesssim 8\pi\left(\frac{y_0}{y_1}\right)^2 \exp(y_1 - y_0) \equiv \delta_1{}^s. \tag{A22}$$

The fraction with two continuum particles satisfies

$$\frac{\Lambda_2}{\Lambda_0} \lesssim \frac{(8\pi)^2}{3}\left(\frac{1}{n_n{}^{\rm nuc}}\right)\left(\frac{m_n y_2{}^2}{2ah^2}\right)^{3/2}\left(\frac{y_0}{y_2}\right)^2 \exp(y_2 - y_0) \equiv \delta_2{}^s. \tag{A23}$$

In general the separation energies for protons and for neutrons are different. Two particle separation energies vary with the constitutents of the pair. The nuclei of interest (cf. § III above) are neutron-rich. Typical neutron separation energies are 3–5 MeV, and those for protons are 16–20 MeV (cf. Table 4 of Garvey *et al.* 1969). Tables 2 and 3 show that for separation energies $\gtrsim$ 16 MeV the levels with energetically separable particle contribute

TABLE 3

UPPER LIMIT δ_2^s ON THE FRACTIONS OF LEVELS WITH TWO PARTICLES FOR VARIOUS NUCLEAR EXCITATIONS AND TWO-PARTICLE SEPARATION ENERGIES ($a = 7$ MeV^{-1})

	E/MeV		
($\Delta_n{}^A + \Delta_n{}^{A-1}$/MeV)	15	25	50
6.....	6.6 (−2)	5.5 (−1)	4.9
8.....	8.9 (−3)	1.5 (−1)	2.1
10.....	8.6 (−4)	3.7 (−2)	9.1 (−1)
12.....	4.7 (−5)	8.4 (−3)	3.8 (−1)
14.....	5.6 (−7)	1.7 (−3)	1.5 (−1)
16.....	0	2.8 (−4)	6.1 (−2)

NOTE.—The density of either protons or neutrons in the nucleus was taken to be one-half of a typical nuclear density ($n_n{}^{\rm nuc} = 6.0 \times 10^{37}$ cm^{-3}).

negligibly to the total level number, even up to excitation energies of 50 MeV. Thus for the nuclei of interest, only states with neutrons above separation energies will be significant. Since the neutron separation energies are 3–5 MeV for these nuclei, the fraction of states with one particle in the continuum is appreciable even at excitation energies as low as 15 MeV. Note that the two-particle $\delta_2{}^s$ becomes comparable to $\delta_1{}^s$ only at very high excitation ($E_A \gtrsim 50$ MeV) and low separation ($\Delta_n{}^A \sim \Delta_n{}^{A-1} \lesssim 4$ MeV) energies.

REFERENCES

Arnett, W. D. 1973, in *Explosive Nucleosynthesis*, ed. D. N. Schramm and W. D. Arnett (Austin: University of Texas Press).

———. 1977, *Ap. J.*, **218**, 815.

Baym, G., Bethe, H. A., and Pethick, C. J. 1971, *Nucl. Phys.*, **A175**, 225.

Bethe, H. A. 1937, *Rev. Mod. Phys.*, **9**, 69.

Bowers, R. L., Gleeson, A. M., and Wheeler, J. W. 1977, *Ap. J.*, **213**, 531.

Bruenn, S. W., Arnett, W. D., and Schramm, D. N. 1977, *Ap. J.*, **213**, 213.

Buchler, J. R., and Coon, S. A. 1977, *Ap. J.*, **212**, 807.

Burbidge, E. M., Burbidge, G. R., Fowler, W. A., and Hoyle, F. 1957, *Rev. Mod. Phys.*, **29**, 547.

Canuto, V. 1974, *Ann. Rev. Astr. Ap.*, **12**, 167.

Chiu, H.-Y. 1968, *Stellar Physics* (Waltham, Ma: Blaisdell).

Clifford, F. E., and Taylor, R. J. 1964, *Mem. R.A.S.*, **69**, 21.

Colgate, S. A., and White, R. H. 1966, *Ap. J.*, **143**, 626.

El Eid, M. F., and Hilf, E. R. 1977, *Astr. Ap.*, **57**, 243.

Fowler, W. A., Engelbrecht, C. A., and Woosley, S. E. 1978, *Ap. J.*, **226**, 984.

Garvey, G. T., Gerace, W. J., Jaffe, R. L., Talmi, I., and Kelson, I. 1969, *Rev. Mod. Phys.*, **41**, S1.

Gilbert, A., and Cameron, A. G. W. 1965, *Canadian J. Phys.*, **43**, 1446.

Hansen, J. P. 1973, *Phys. Rev. A*, **8**, 3096.

Karpov, K. A. 1965, *Tables of the Function* $W(Z) = e^{-Z^2}\int_0^Z e^{x^2}dx$ *in the Complex Domain* (New York: Macmillan).

Lamb, D. Q., Lattimer, J. M., Pethick, C. J., and Ravenhall, O. G. 1979, in preparation.

Lattimer, J. M., and Ravenhall, O. G. 1978, *Ap. J.*, **223**, 314.

Mackie, F. D. 1976, Ph.D. thesis, University of Illinois at Urbana-Champaign.

Mazurek, T. J. 1976, *Ap. J.* (*Letters*), **207**, L87.

———. 1979, in preparation.

Tubbs, D. L. 1978, *Ap. J. Suppl.*, **37**, 289.

Wilson, J. R. 1977, Varenna Lectures, in press.

Yueh, W. R., and Buchler, J. R. 1977, *Ap. J.* (*Letters*), **211**, L121.

G. E. Brown: State University of New York at Stony Brook, Stony Brook, NY 11794

James M. Lattimer: Department of Astronomy, University of Illinois, Urbana, IL 61801

T. J. Mazurek: Nordita, Blegdomsvej 17, DK-2100 Copenhagen, Denmark